Laboratori Nazionali di Frascati

ON PROTON MULTIPLE INELASTIC NUCLEAR INTERACTIONS IN BENT CRYSTALS

Anton Babaev[1,2], Sultan Dabagov[2,3]

[1] *Tomsk Laboratory of Computational Physics, 634050 Tomsk, Russia*
[2] *INFN-Laboratori Nazionali di Frascati Via E. Fermi 40, I-00044 Frascati, Italy*
[3] *RAS P.N. Lebedev Physical Institute & National Research Nuclear University, Moscow, Russia*

Abstract

The probability of inelastic nuclear interactions is studied for relativistic channeled and quasi-channeled protons in a bent crystal. Multiple passage of projectiles through experimental setup was in details considered. Simulation results were compared with known experimental ones, paying attention to the features observed.

PACS.: 61.85+p; 02.60.Cb

1 Introduction

As known, channeled and quasi-channeled projectiles move under small angles to main crystallographic planes (we consider the planar channeling here) and they actually interact with the averaged field of planes' atoms instead of the fields of separate atoms (see, for example, [1] and Refs. therein). The channeling phenomenon takes place when incident angle θ_0 between projectile velocity and crystallographic planes does not exceed the certain critical value θ_L (so called Lindhard angle). Channeled projectiles penetrate into the crystal at angles $\theta_0 < \theta_L$ and they move between two parallel planes forming a planar channel. If the angle between initial velocity and planes is over than critical one but remains close to its value, the quasi-channeling regime takes place. Hence, quasi-channeled projectiles are not constrained with any single channel.

In the case of bent crystal the effective crystal field is axial. It depends on the distance to the center of bending curvature (see [2–4] for details). The projectile's beam directed along the bent planes at either channeling or quasi-channeling conditions is split onto two beams in the crystal. The first beam is channeled and might be deflected along bent channel through large angles from the initial direction of motion. The second beam is quasi-channeled. For quasi-channeled particles that move initially to the center of crystal curvature the volume reflection can be observed. Namely, in the trajectory we can define a "turn" point where the particle starts moving "from the center of crystal curvature". That results in reflected beam deflection by crystal field in the opposite direction to that for channeled particles. Quasi-channeled particles initially moving from the center of curvature might be slightly deflected mainly due to multiple scattering on crystal nuclei. Obviously, multiple scattering can result in transition of projectiles between channeled and quasi-channeled states; the phenomena observed are known as dechanneling and volume capture in oriented crystals.

This work aims in studying the probability of inelastic nuclear interactions (INI) for both channeled and quasi-channeled protons in a bent crystal. Namely, we have evaluated the scattering of 120 GeV protons in a Si crystal bent along (220) crystallographic planes at the angle $\alpha_R = 150\,\mu$rad with the radius $R = 1333$ cm ; the crystal thickness is $z_{cr} = 2$ mm; the critical channeling angle for this case is $\theta_L = 19\,\mu$rad (the conditions of experiment [5]).

We have introduced in considerations the averaged probability of INI and, successfully, evaluated its dependence on the crystal orientation. A special attention has been payed to the features of projectile multiple passage of the crystal. Suggesting the model of experimental scheme [5], a mathematical code enabling the description of these features has been developed.

2 Averaged probability of INI

2.1 Theoretical consideration

Let designate σ for the INI cross-section. The INI probability when proton passes the way z in amorphous solid is $P = \sigma N z$ (which is valid if $P << 1$) where N is the nuclear density [1]. In aligned crystal, for both channeling and quasi-channeling conditions, the nuclear density N strongly depends on the distance from crystallographic planes due to the thermal vibrations of nuclei near the equilibrium position located on a plane. Let use the Gaussian distribution for the displacement of nuclei from the plane [1]. Then for aligned crystal the INI probability can be rewritten as follows:

$$P = \sigma \langle N \rangle_{tr} z \,,$$

where $\langle N \rangle_{tr}$ is the averaged nuclear density over the projectile trace.

Now let consider nondivergent proton beam hitting the bent crystal at the incident angle θ_0 (see, for details, in [3,4] and Refs. therein). To define the mean (averaged) nuclear density $\langle N \rangle_0$ for incident beam at given crystal orientation (which is defined by the angle θ_0) we have to average $\langle N \rangle_{tr}$ by all proton trajectories.

Assuming that the number of protons penetrating into the crystal is large, $n_p >> 1$, we should not analyze the trajectory for each proton, but can define that the averaged INI probability in a crystal volume is

$$P = \sigma \langle N \rangle_0 z \tag{1}$$

for one arbitrary proton, and the full number of nuclear reaction as $Z = P n_p$.

Hence, if the counter (detector) is mounted anywhere near the crystal for the nuclear reaction registration, it records the quantity proportional to the value Z.

2.1.1 *Simulations and discussions*

To simplify the analysis, in this subsection, evaluating the proton trajectory, we omit multiple scattering [2].

First of all, let present the change of Si nuclear density N along the proton trajectory at planar channeling (Fig. 1c,d) as well as at volume reflection (Fig. 1a,b). Namely, the nuclear densities are presented in bottom figures whereas in top figures corresponding trajectory sections are shown. Trajectories were evaluated by the algorithm described in [3,4]. It is convenient to simulate the trajectory in axial coordinates (r, φ); hence, the trajectory is situated in the plane orthogonal both to the axis of field symmetry and to bent crystallographic planes. The radial coordinate r originates from the center of the bent planar channel where proton penetrates into the crystal. The azimuth angular coordinate φ is counted from the crystal entrance face. The pole of the coordinate frame

---

[1]The density in this manuscript coincides with the concentration

[2]As shown in Section 3, multiple scattering does not influence significantly the averaged probability (1)

3

is the point where the plane of trajectory crosses the axis of field symmetry. The proton motion in a crystal field is determined by its kinetic energy, incident angle θ_0 and initial radial coordinate r_0.
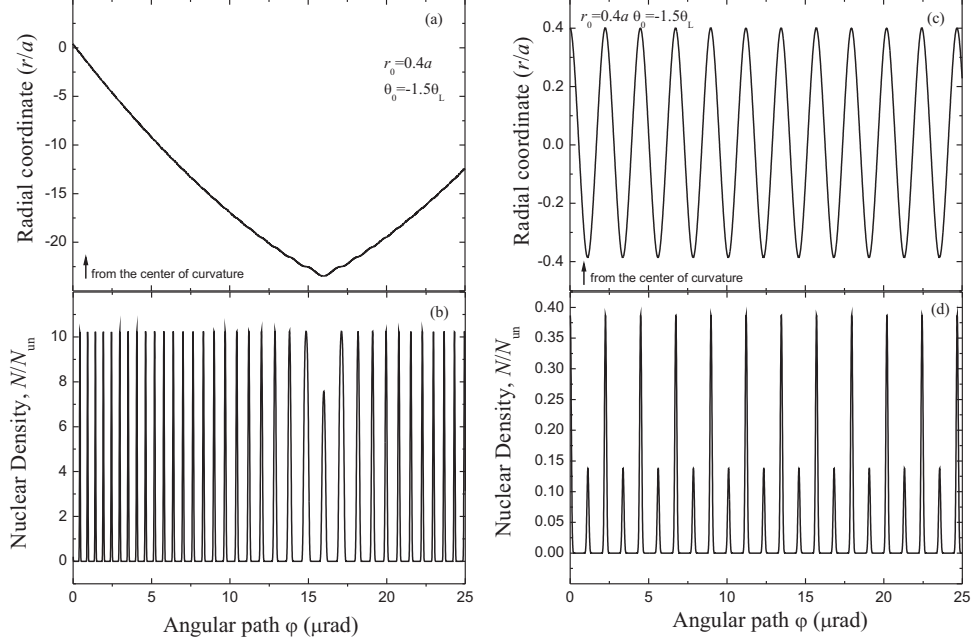

Figure 1: Changes of nuclear density N (b,d) along the initial section of 120 GeV proton trajectories (a,c) in Si crystal bend along (220) planes with the radius $R = 1333$ cm; a is the distance between (220) planes.

In Fig. 1 the nuclear density for unaligned (misaligned) Si crystal $N_{un} = 0.05 \cdot 10^{24}$ cm^3 is introduced to clarify the difference between oriented and unaligned cases. In the condition of volume reflection (Fig. 1a,b) the nuclear density is one order more than N_{un} at proton cross of crystallographic planes. When proton reaches the point of reflection (near $\varphi = 16\,\mu$rad in Fig. 1a) one can see the peak in Fig. 1b smaller than other ones. That takes place due to the fact that proton does not cross the plane at reflection. On other hand, near the plane of reflection proton moves with small radial velocities, and interacts longer than with other planes; and that is the reason of corresponding peak broadening with respect to other peaks. In the channeling condition (Fig. 1c,d) the nuclear density is less than N_{un}. However, when proton approaches bent planes, the nuclear density sharply increases. In a bent crystal the channeled proton is governed by the potential having different barrier heights. Proton can approach a smaller barrier at closer distances than those for a higher barrier, that might result in essentially higher proton-nuclear interaction for the first case than for the second one. The latter explains the fact that in Fig. 1d the curve is composed of alternating small and large peaks.

Finally, let point out here that the averaged nuclear density over the whole trajectory $\langle N \rangle_{tr} / N_{un}$ (i.e. over the angular path $\varphi = \alpha_R$) equals 1.12 for reflected proton and 0.04 for channeled proton.

4

The dependence of averaged over trajectory nuclear density $\langle N \rangle_{tr}$ on the initial point of trajectory r_0 is presented on Fig. 2. The result has distinguished two regimes of the motion: volume reflection for all protons (Fig. 2a) and channeling for majority of protons (Fig. 2b). The averaged nuclear density $\langle N \rangle_{tr}$ for reflected protons (in Fig. 2a) always exceeds the value N_{un}. The peaks in Fig. 2a correspond to protons reflected by one crystallographic plane. Indeed, proton initial radial energy [4] increases at the shift of initial transverse coordinate r_0 from the center of channel. Hence, corresponding protons can closer approach the plane before the reflection, and nuclear density $\langle N \rangle_{tr}$ becomes higher.

On the contrary, at energies higher than potential barrier protons are reflected by successive potential barrier, being more distant from the plane that, in turn, leads to nuclear density $\langle N \rangle_{tr}$ decrease. This feature corresponds to the deep after sharp peak in Fig. 2a.

Channeled protons move in central area of the channel and corresponding averaged nuclear density $\langle N \rangle_{tr}$ (Fig. 2b) is less than the value N_{un}. For channeled protons, which penetrate into the crystal at large distances from the channel center (at $r_0 \approx \pm 0.4a$), the averaged nuclear density $\langle N \rangle_{tr}$ is much higher than for those penetrating near the channel center. Protons penetrating into the crystal with the initial radial coordinates $r_0 \approx 0.5a$ are quasi-channeled (see, in [3,4] for details). The averaged nuclear density $\langle N \rangle_{tr}$ for these protons slightly exceeds the value N_{un}, as in the case of quasi-channeled reflected protons (Fig. 2a). Indeed, proton moves in the area with very high nuclear density N at almost tangent line to the planes; this situation takes place for reflected protons near the reflection point (Fig. 2a) as well as for quasi-channeled protons with trajectories characterized by $\theta_0 = 0$ at the initial trajectory section (in Fig. 2b).

The evaluation gives us the averaged nuclear density at given crystal orientation $\langle N \rangle_0$ that results in $\langle N \rangle_0 / N_{un} = 1.12$ for the case of Fig. 2a and 0.19 at the Fig. 2b conditions.

The results of Fig. 2 allows us to conclude that the main contribution to INI is expected from the channeled protons making the oscillations with the extreme possible amplitudes in the channel (that proves the earlier results and conclusions by other authors [6]). Here, it should be underlined that the proton dechanneling becomes evident.

Now we can evaluate the dependence of averaged nuclear density $\langle N \rangle_0$ on the crystal orientation, i.e. on the angle θ_0 between proton velocity and bent crystallographic planes at the crystal entrance end. The results of simulations are presented in Fig. 3. Let define $\theta_0 > 0$ for projectiles moving from the center of curvature initially, and $\theta_0 < 0$ - in opposite case. The value $\theta_0 = 0$ corresponds to a projectile penetrating into the crystal strongly along the tangent line to bent planes at crystal entrance end (see [3,4] for details). Namely, in Fig. 3a the averaged nuclear densities $\langle N \rangle_0$ are shown, whereas the corresponding INI probability P (1) is presented in Fig. 3b. The cross-section $\sigma = 0.506 \cdot 10^{-24}$ cm^2 was taken from [6]. When the parallel proton beam is directed initially along the crystallographic planes (the channeling orientation, CO) the probability of nuclear interaction is five times reduced in comparison to one in unaligned crystal orientation (UAO). This result is in agreement with the experimental data [5]. At the conditions of volume reflec-
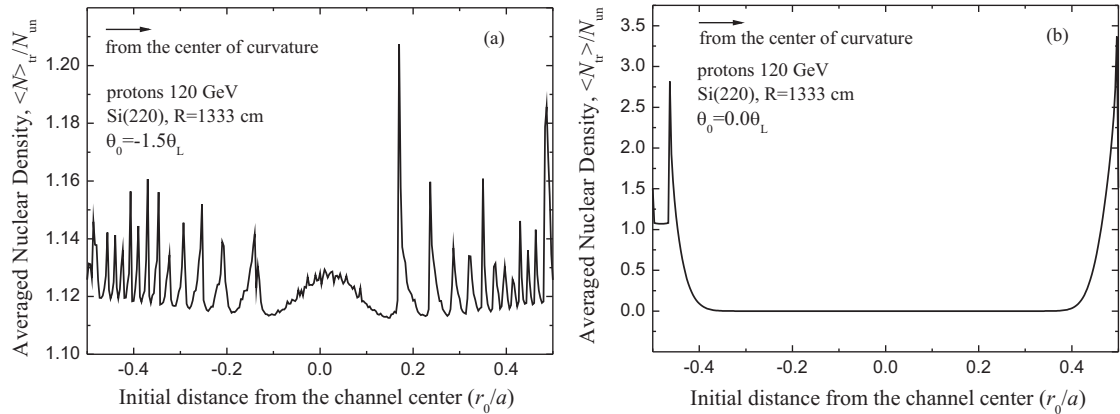
Figure 2: Averaged nuclear density $\langle N \rangle_{tr}$ over proton trajectory in dependence on the point r_0 of penetration into the channel: a) volume reflection conditions, b) channeling conditions. The case of 120 GeV protons passing through Si crystal bent along (220) planes over the angle $\alpha_R = 150\,\mu$rad with the radius $R = 1333$ cm is considered.

tion (volume reflection orientation - VRO in Fig. 3), the INI probability is $\sim 10\%$ higher than in UAO. The authors of [6] came to the similar conclusion. On other hand, the experimental curve in [5] for the condition of volume reflection appears below the curve for unaligned crystal orientation. As further shown this effect is related to the particles multiple passage through the experimental setup. When crystal is aligned for the optimum of UAO, the relation $\langle N \rangle_0 / N_{un}$ approaches the unity and the INI probability aims asymptotically to the constant value. It is notable that in a whole considered interval of the angles θ_0 the INI probability is less than 1%.

3 Multiple passage of projectiles through bent crystals

3.1 Theoretical description

3.1.1 The idealized experimental setup

In experiments [5,6] the holder with bent crystals was mounted into the pipe of storage ring, resulting in the projectile multiple passages through the setup. Obviously, the INI value should vary in comparison with a single passage case above examined. On one side, multiple passage of a projectile through the crystal should be characterized by similar features we can observe with the crystal thickness increase, i.e. one can expect the growth of the INI number. On other side, projectiles might be large deflected from its initial direction of motion due to both channeling and volume reflection effects, and, finally, projectiles can leave the portion of a beam hitting a crystal. As the result, the deflection of particles might restrict the growth of INI number in multiple passage regime.

To model the situations described above, let consider a simple idealized experimental scheme (see in Fig. 4). A parallel beam 1 maintains one bunch containing initially
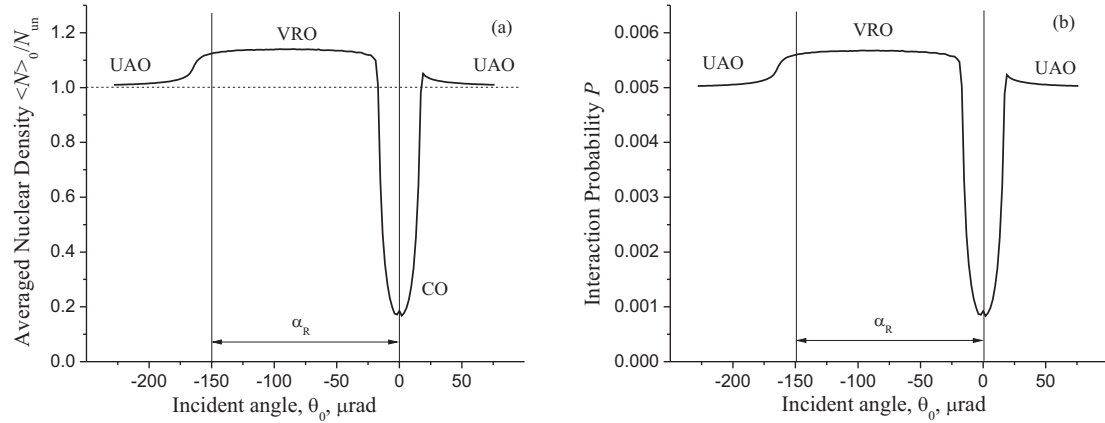
6

Figure 3: Dependence both of the averaged nuclear density $\langle N \rangle_0$ (a) and of the INI probability P (b) on the incident angle θ_0. The case of 120 GeV protons passing through Si crystal bend along (220) planes over the angle $\alpha_R = 150\,\mu$rad with the radius $R = 1333$ cm is considered. The designations in the figure are: UAO – unaligned orientation, when the deflection of protons is determined mainly by multiple scattering; VRO – volume reflection orientation, when the deflection of protons is determined mainly by the volume reflection; CO – channeling orientation, when the deflection of protons is determined mainly by the channeling.

the number $I_0 >> 1$ of protons. The absorber system 5 are placed to cut the tails of a beam. The focusing system 6 is mounted behind the absorber. Keeping the beam profile, it delivers the beam to the setup entrance. Let mount the bent crystal 2 into the beam before the absorber 5; the number αI_0 of protons hits the crystal. Hence, particles can be deflected from the initial direction due to channeling 3 or volume reflection 4 at large angles exceeding the cutting value θ_b. These particles cut by absorber 5 will leave the beam. Other particles, namely, which either did not hit the crystal or being deflected at angles less than the cutting angle θ_b, pass to the focusing system 6. The focusing system makes the beam parallel again and restores initial beam profile. After that steered beam is turned to the crystal collimation setup.

Let introduce coefficient β defining the part of protons hitting the crystal and being deflected by bent crystal on the angles $|\theta| < \theta_b$. Namely, coefficient β is the part of protons crossing the crystal and successfully passing to the focusing system. Coefficient β can be evaluated from the angular distribution by the earlier developed method [3]. While the focusing system restores the beam profile, the coefficient β remains unchanged from the turn to turn. This coefficient depends on crystal orientation (i.e., on the angle θ_0). Also, both coefficients α and β, being independent on the number of beam turns, correspond to both orientation and position of a crystal.
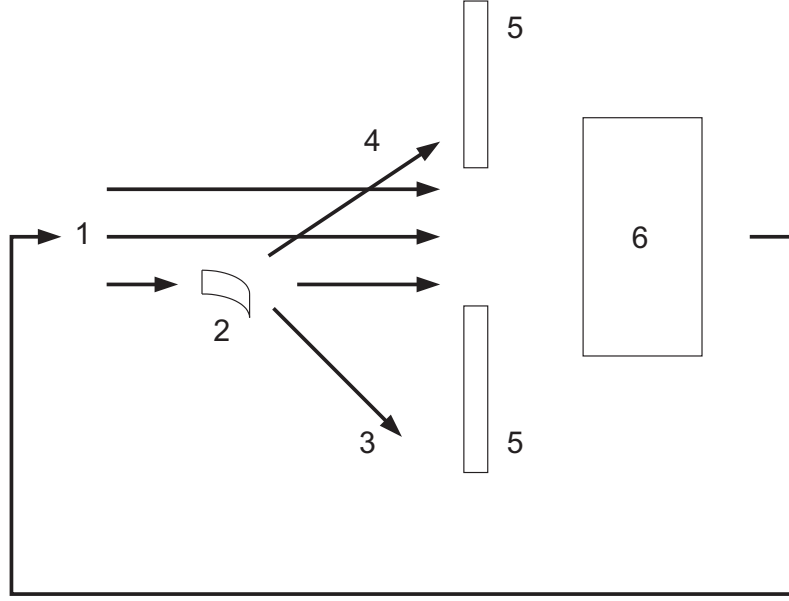
7

Figure 4: Experimental setup scheme: 1 – the initial parallel proton beam, 2 – the bent crystal, 3 – the channeled protons, 4 – the reflected protons, 5 – the absorber, 6 – the focusing system.

3.1.2 The dependence of the protons number on the number of turns

Let now define dependence for particles number in a beam on the number of turns under the INI neglecting condition.

The first turn is considered. The number of particles in the beam is $I_{0,1} = I_0$ at the experimental setup entrance. The number of particles hitting the crystal is αI_0. The part of these particles that passes to the focusing system is defined by $\alpha\beta I_0$. Therefore, the full number of particles at the focusing system entrance is $I_{t,1} = (1 - \alpha) I_0 + \alpha\beta I_0$.

The second turn is considered. The number of particles in the beam $I_{0,2} = I_{t,1}$. The number of particles hitting the crystal is $\alpha I_{0,2}$. The part of these particles passing to the focusing system is now $\alpha\beta I_{0,2}$. Therefore, the full number of particles at the focusing system entrance is $I_{t,2} = (1 - \alpha + \alpha\beta) I_{0,2} = (1 - \alpha + \alpha\beta)^2 I_0$.

For the T-th turn one can obviously obtain that the number of particles in the beam is $I_{0,T} = (1 - \alpha + \alpha\beta)^{T-1} I_0$. Therefore, the full number of particles entering the focusing system is $I_{t,T} = (1 - \alpha + \alpha\beta)^T I_0$.

3.1.3 The INI estimation

Let now consider the problem of INI in the crystal volume. As shown in Section 2 the INI probability is quite small for one proton during the single passage through the crystal. Therefore, the proton leaving the beam due to INI does not affect the full number of

8

particles and expressions above are valid for the INI evaluation over T turns.

For the 1st turn the number of particles hitting the crystal is αI_0, while the number of nuclear reactions is defined as $Z_1 = P\alpha I_0$. Then for the 2nd turn the number of particles hitting the crystal will be $\alpha I_{0,2} = \alpha \left(1 - \alpha + \alpha\beta\right) I_0$, and successfully the number of nuclear reactions - $Z_2 = P\alpha I_{0,2} = P\alpha \left(1 - \alpha + \alpha\beta\right) I_0$. Further, the 3rd turn will be characterized by the number of particles hitting the crystal $\alpha I_{0,3} = \alpha \left(1 - \alpha + \alpha\beta\right)^2 I_0$, and, correspondingly, by the number of nuclear reactions $Z_3 = P\alpha I_{0,3} = P\alpha \left(1 - \alpha + \alpha\beta\right)^2 I_0$.

Hence, we can define $Z_T = P\alpha \left(1 - \alpha + \alpha\beta\right)^{T-1} I_0$ for the T-th turn, and the full INI number over T turns as follows

$$Z = \sum_{i=1}^{T} Z_i = P\alpha I_0 \sum_{i=1}^{T} \left(1 - \alpha + \alpha\beta\right)^{i-1}.$$

The sum in the last expression actually represents the geometrical progression with the first term equal to 1 and denominator $q = (1 - \alpha + \alpha\beta)$. Assuming the crystal does not accept the beam completely, one can estimate $\alpha < 1$. Additionally, the coefficient $\beta < 1$, if the absorber cuts protons, whereas the value $\beta = 1$ corresponds to the case when all protons pass to the focusing system.

Therefore, at $\beta < 1$, we have $q < 1$ and in this case

$$Z = \frac{1 - (1 - \alpha + \alpha\beta)^T}{1 - \beta} P I_0. \tag{2}$$

For the case $\beta = 1$ one can find that

$$Z = TP\alpha I_0. \tag{3}$$

Indeed, when all particles pass to the focusing system the full number of particles does not change while condition $Z_i << I_{0,i}$ is fulfilled. Hence, the formula (3) concludes that in each turn the same number of particles αI_0 hits the crystal, and the same number of reactions $P\alpha I_0$ takes place.

On the contrary, as follows from Eq.(2) when number of turns increases the full number of nuclear reactions Z reaches saturation characterized by the following limit

$$Z_{\mathrm{inf}} = \frac{P}{1 - \beta} I_0. \tag{4}$$

The obtained result is α independent. As the matter of fact, α defines the time to reach the saturation. Indeed, the coefficient α is the part of a beam hitting the crystal, and it depends on the crystal position with respect to the beam center. However, the saturation appears at any crystal position in the limit $T \to \infty$.

To estimate the number of turns when the saturation can be reached, let define the value η, which characterizes the difference between the numbers of INI at saturation Z_{inf} (4) and for limited number T of turns Z (3):

$$\eta = 1 - \frac{Z}{Z_\infty} = \left(1 - \alpha + \alpha\beta\right)^T.$$

9

From this definition one can obtain the relation

$$T = \frac{\ln \eta}{\ln (1 - \alpha + \alpha\beta)}. \tag{5}$$

For example, let choose the cutting angle $\theta_b = 10$ μrad in order to estimate the number of turns T necessary to get $\eta = 0.01$ at the value $\alpha = 0.05$, and previously defined parameters of both crystal and beam (see, in Introduction). If the incident angle $\theta_0 = 0$ (the channeling orientation) one can obtain the angular distribution (the model by [3]), and then we can define $\beta = 0.05$. Using this data one can find $T = 95$ from Eq.(5). For the case of incident angle $\theta_0 = -1.5\theta_L$ (volume reflection orientation) we obtain $\beta = 0.17$, and at the same value $\eta = 0.01$ - the number of turns $T = 109$. Actually, the saturation is established very rapidly at given $\alpha = 0.05$.

3.2 Simulation results

To eliminate the dependence on crystal position (i.e., on coefficient α) we will consider further the INI number in the saturation regime. From considerations above one can conclude the INI number depends on both incident θ_0 and cutting θ_b angles. It should be underlined that the coefficient β is strongly correlated with the angular distribution shape of protons crossed the crystal, and the multiple scattering of protons [7,8] has to be included in the evaluation.

   In that case the INI probability P is shown in Fig. 5. Taking into account the multiple scattering smoothes out the transition from VRO to UAO in comparison with the curve presented in Fig. 3b (without multiple scattering features).
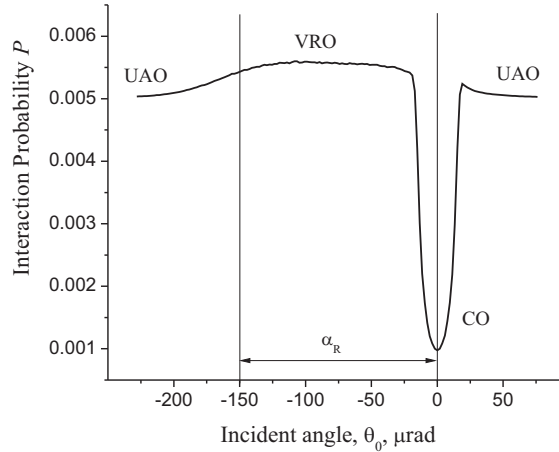

Figure 5: The same as in Fig. 3b, but with multiple scattering of protons

   The dependences $\beta\left(\theta_0\right)$ at different cutting angles θ_b are presented in Fig. 6 where to higher curve by the position in a figure corresponds larger angle. To clarify the nature

of curves β in Fig. 6, several angular distributions are presented in Fig. 7 [3]. The part of angular distribution placed between the vertical identical-color lines corresponds to protons passed to the focusing system at the given cutting angle θ_b. Actually, the coefficient β is the ratio of the integral intensity between identical-color lines to the total intensity in the graph. The angular distribution in Fig.7a is obtained in the CO condition, whereas in Fig. 7b - for the VRO case. The angular distribution in Fig. 7c corresponds to the transition area from VRO to UAO ($\theta_0 \approx -\alpha_R$).
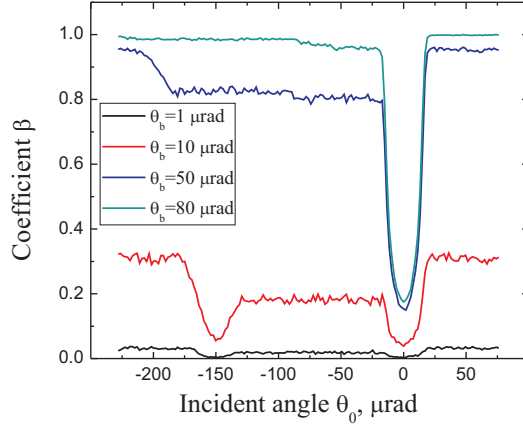

Figure 6: The coefficient β as the function of the incident angle θ_0 at different cutting angles θ_b. The case of 120 GeV protons passing through Si crystal bend along (220) planes over the angle $\alpha_R = 150\,\mu$rad with the radius $R = 1333$ cm is considered.

All curves in Fig. 6 are revealed the deep in CO area. Indeed, channeled projectiles are deflected by bent crystal at large angles $\theta \approx -\alpha_R < -\theta_b$. Hence, all channeled particles hit the absorber and leave the beam.

Black lines (at small θ_b) of the figure 7 compose only small part of total distribution, and it reveals a slight variation at angular distribution change (i. e. θ_0). Therefore, the corresponding curve in Fig. 6 is the lowest, and the coefficient β changes slightly.

On the contrary, between green lines in Fig. 7 (at the largest angle θ_b) almost whole distribution situates at any crystal orientation except CO. All protons pass to focusing system except the crystal orientation when the majority of projectiles are channeled and deflected at the angles $|\theta| > \theta_b$. Therefore, one can expect $\beta \approx 1$ except the sharp decrease in CO, as shown in Fig. 6.

For intermediate angles $\theta_b = 10\,\mu$rad and $50\,\mu$rad the coefficient β in Fig. 6 demonstrates quite different behavior. Namely, for the case $\theta_b = 10\,\mu$rad one can see the deep in the area $\theta_0 \approx -\alpha_R$ whereas for the case $\theta_b = 50\,\mu$rad this deep is absent. To understand this difference one should pay the attention to Figs. 7b,c. The intensity integrals between blue lines ($\theta_b = 50\,\mu$rad) are approximately the same in these figures, whereas in the case

---

[3]The modified model of [3], in which multiple scattering has been included; details will be published elsewhere.
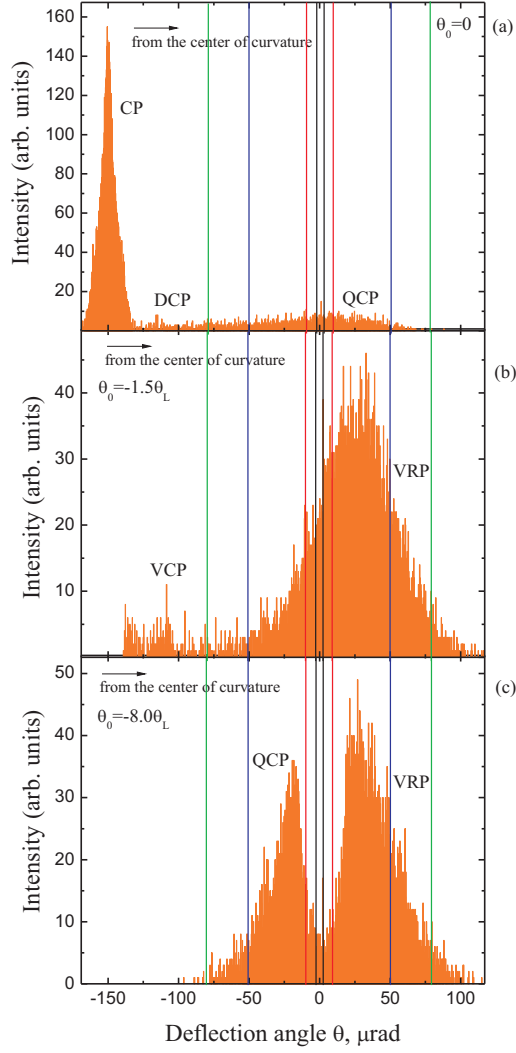
Figure 7: Angular distributions of 120 GeV protons passing through the Si crystal bend along (220) planes over the angle $\alpha_R = 150\,\mu$rad with the radius $R = 1333$ cm. The incident angles are: a) $\theta_0 = 0$, b) $\theta_0 = -1.5\theta_L$, c) $\theta_0 = -8\theta_L$. The part of angular distributions located between the vertical lines of identical color defines the number of protons passing to the focusing system at different angles θ_b: black lines - $\theta_b = 1\,\mu$rad, red lines $\theta_b = 10\,\mu$rad, blue lines - $\theta_b = 50\,\mu$rad, green lines - $\theta_b = 80\,\mu$rad (these designations correspond to colors in Fig. 6). The fractions in the outgoing beam are: CP – channeled protons, VRP – quasi-channeled protons, which suffer the volume reflection, QCP – quasi-channeled non-reflected protons, which deflect due to multiple scattering only, DCP – dechanneled protons, VCP – quasi-channeled protons, which suffer the volume capture (see, in [9] for details). The angles $\theta < 0$ correspond to the deflection to the center of curvature, whereas, on the contrary, the angles $\theta > 0$ - from the center of curvature (see [3,4] for details).

12

of red lines ($\theta_b = 10\,\mu$rad) the integral in Fig. 7c is less than in Fig. 7b. Therefore, at the angular scan by θ_0 and transit from VRO to UAO, the β difference at $\theta_b = 50\,\mu$rad is not evident. On the contrary, one can obtain the decrease in coefficient β at $\theta_b = 10\,\mu$rad. Actually, when crystal is mounted in VRO, the majority of protons forms a single sharp peak. This peak is scanned at both $\theta_b = 50\,\mu$rad and $\theta_b = 10\,\mu$rad. When crystal is mounted at angle $\theta_0 \approx -\alpha_R$, outgoing beam is split onto two beams. One part of projectiles moves under volume reflection condition whereas other part is mainly deflected due to multiple scattering. The observer watching the projectiles behind the absorber (at the entrance to the focusing system) scans both peaks at $\theta_b = 50\,\mu$rad simultaneously, i.e. he observes the same intensity of projectiles as in the VRO area. But at the condition $\theta_b = 10\,\mu$rad the observer registers one peak only or even the deep between peaks (as in Fig. 7c). As the matter of fact, the number of particles passing to the focusing system decreases with respect to VRO.

Both dependencies $\beta\,(\theta_0)$ (Fig. 6) and $P\,(\theta_0)$ (Fig. 5) define the INI number in the crystal volume (4). The number Z_{inf} is presented in Fig. 8 for the same conditions as for the coefficient β in Fig. 6. The cutting angle θ_b increases from Fig. 8a to Fig. 8d. For all parts of Fig. 8 the deep in the CO appears. It is caused by the deflection of channeled protons at large angles (see, in Fig. 6) as well as by the reduce of the INI probability (see, in Fig. 5). The INI number in VRO becomes larger with the increase of angle θ_b. It proves the expectation: the more this angle the more protons pass many times through the crystal.

In Fig. 8a the cutting angle is very small ($\theta_b = 1\,\mu$rad). Therefore, every proton passes through the crystal one time only and after that it is deflected by the crystal to the absorber. In this case the ratio of nuclear interaction number Z_{inf} to the full number of projectiles I_0 is, actually, the INI probability P for one proton (Fig. 5).

In Fig. 8b ($\theta_b = 10\,\mu$rad) one can see the deep in the area $\theta_0 \approx -\alpha_R$ whereas the similar deep is absent in Fig. 8c ($\theta_b = 50\,\mu$rad) that agrees with the $\beta\,(\theta_0)$ analysis above presented.

At the cutting angle $\theta_b = 80\,\mu$rad (Fig. 8d) the number of protons, which suffer the INI, is about 40% from its initial number I_0 in VRO, and this number approaches 100% in UAO. It should be underlined that here the saturation state has been considered. Obviously, to distinguish these quantities the huge number of turns is needed.

Let now explain the sharp oscillations of the curves Z_{inf}/I_0 in Figs. 8c,d. One can notice from Fig. 6, the coefficient β in the corresponding areas is 0.98-0.99. Further, as follows from Eq.(4), the small variation in the coefficient β leads to significant change of the INI number Z_{inf}. The coefficient β is determined by the shape of corresponding angular distribution. Hence, the small change of the distribution shape results in large variations of the INI number at cutting angles closed to the half of the full angular distribution width. On the one hand, actually, the distribution shape changes at different crystal orientations. On the other hand, the Monte-Carlo method used in our simulations to obtain the angular distribution can also contribute to small variation of the distribution shape. Both contributions form the final oscillations in UAO shown in Fig. 8c as well as in VRO shown in Fig. 8d.
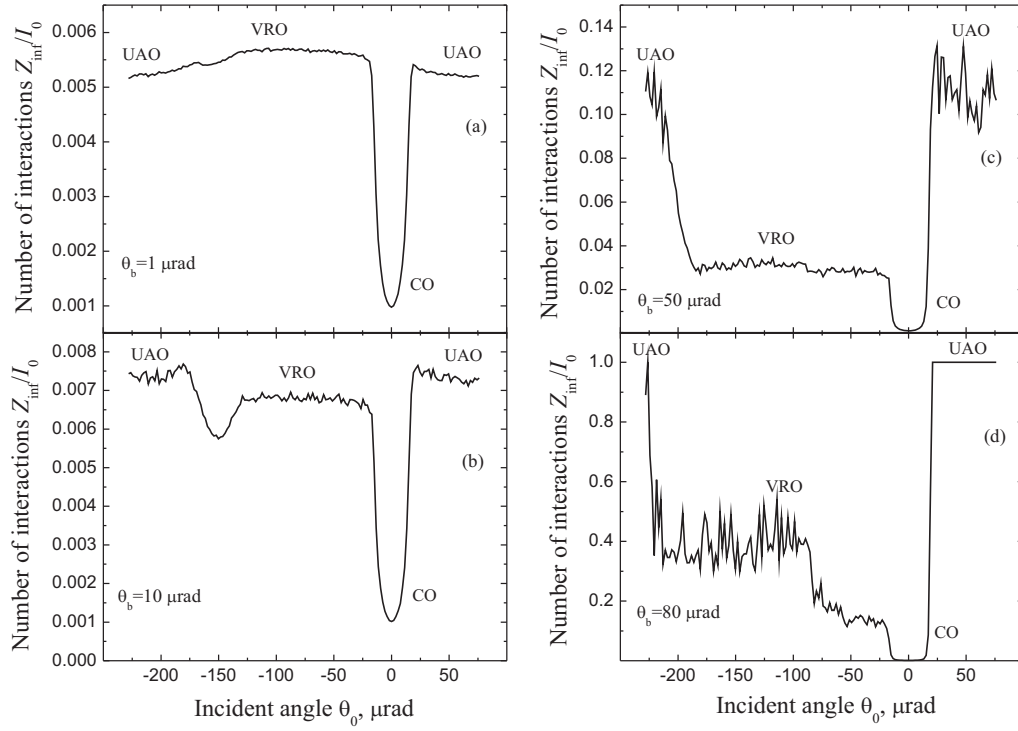
Figure 8: The INI number for the saturation state Z_{inf} with respect to the initial number of protons I_0 in dependence on the incident angle θ_0 at different cutting angles θ_b: a) $\theta_b = 1\,\mu\mathrm{rad}$, b) $\theta_b = 10\,\mu\mathrm{rad}$, c) $\theta_b = 50\,\mu\mathrm{rad}$, d) $\theta_b = 80\,\mu\mathrm{rad}$. The case of 120 GeV protons passing through Si crystal bend along (220) planes over the angle $\alpha_R = 150\,\mu\mathrm{rad}$ with the radius $R = 1333$ cm is considered.

For the range $\theta_0 = -75^o \div -25^o$ there is an interval in VRO area in Fig. 8d where the sharp oscillations are absent. These crystal orientations are characterized by significant deflection ($\theta > \theta_b$) of protons due to the volume capture effect [9]. As the result, a few percents of protons leave the beam and small changes of the distribution shape does not significantly influence the INI number (see, in Fig. 7c).

At UAO the deflection of projectiles is defined by multiple scattering mainly at angles $\theta < \theta_b$. Therefore, in this area the coefficient $\beta = 1$ (Fig. 6 and Fig. 8d). As above shown the saturation effect does not exist in that case. One can suppose that all protons will suffer the nuclear interactions in the limit $T \to \infty$, as it is shown in Fig. 8d. Nevertheless, in the practice, one can not reach the ratio $Z/I_0 \approx 1$ due to the small P value, huge number of turns, damaging of the crystal, etc.

The INI number tends to 1 in the VRO area at the large cutting angle (Fig. 8d), whereas it remains stable in VRO at other considered cutting angles. This is related to the decrease of the full distribution width when incident angle θ_0 changes from $-\theta_L$ to $-\alpha_R$ (see [9] for details). Indeed, as known [3,4,9], the position of reflected protons peak does not depend on the incident angle θ_0, whereas the tail length for captured protons (see, in Fig. 7b and [9,10]) decreases together with the incident angle change. Therefore, at angle $\theta_b = 80\,\mu$rad more and more captured protons reach the focusing system, when the incident angle is changed by the way pointed out above. As a result, the number of interactions increases. At the same time, the number of protons passing to the focusing system at other considered angles $\theta_b < 80\,\mu$rad does not changes significantly. At these angles reflected protons pass to the focusing system whereas captured protons are deflected at angles $|\theta| > \theta_b$ (see, in Figs. 7b). Hence, the number of passing protons does not depend significantly on the incident angle, and the INI number remains stable at VRO.

Finally we consider the next feature of obtained results. When projectiles pass through the crystal one time, the INI probability is more at VRO than at UAO (see, Fig. 5 and Fig. 8a). When the turn's number increases, on the contrary, this probability is more at UAO than at VRO (Fig. 8(b-d)). Actually, taking into account the multiple passage of projectiles through the crystal changes qualitatively the crystal orientation where maximal INI intensity appears. Indeed, at UAO protons are deflected on the fewer angles with respect to the case of VRO (see discussion above and [9]). Therefore, a proton has a chance to make more turns before it will be deflected by the angle $\theta > \theta_b$ at UAO than at VRO. Due to the fact that the probability of interaction growths with the increase of the number of turns, at multiple passage we will have the reduced INI probability at VRO with respect to UAO. This result is in agreement with [5,6]. In Fig. 9 this effect is illustrated: the INI number defined by expression (2) initially is more in the VRO than in the UAO, but the situation becomes inverted starting from the 5-th turn. Also, in Fig. 9 one can see the evolution of saturation effect.

Conclusion

In this work we have considered the probability of inelastic nuclear interactions when relativistic protons pass through the bent crystal. The main attention was paid to the mul-
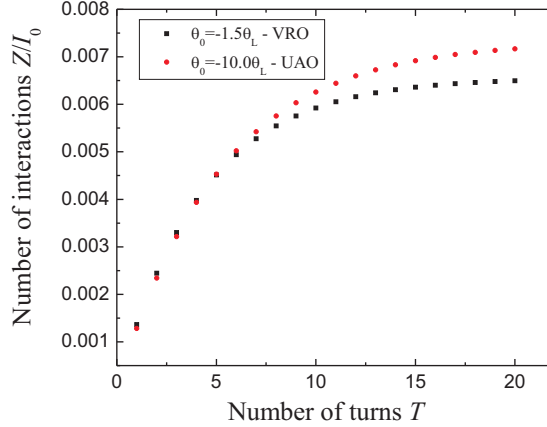
Figure 9: INI number Z with respect to the initial number of protons I_0 as the function of the turns number T at $\alpha = 0.25$, $\theta_b = 10\,\mu\text{rad}$. The case of 120 GeV protons passing through Si crystal bend along (220) planes over the angle $\alpha_R = 150\,\mu\text{rad}$ with the radius $R = 1333$ cm is considered.

tiple passage of protons through the experimental setup. The idealized experiment was simulated to investigate the INI for these conditions. The scheme of experiment involves both a bent crystal to deflect the projectiles and an absorber to cut-off the deflected particles. These are main elements used in real accelerator technique to collimate the charged particles beam. The suggested setup (idealized for simplicity), in general, works as a real collimator facility. At the same time, this theoretical experiment abstracts from the technical details making the experimental data nature not so clear. Hence, our idealized setup can be used to better understand the real experimental features.

Presented analysis enables explaining the difference between experimental data and results of simulations published in [5]. The published data are not adapted for direct analysis. Nevertheless, the shape of our simulated curves in Fig. 8 is in qualitatively agreement with the data [5]. Additionally, we would like to underline that the developed model allowed us to explain observed deeps in the INI counts when the crystal is mounted in the transition area from volume reflection to unaligned crystal orientation. Actually, it is not related to inelastic interactions themselves. It is purely the effect of the beam collimation. The mentioned deep can be either enhanced less or more or can be even absent in dependence on the cutting angle at the setup exit.

The oscillations at both VRO and UAO discussed above might be smoothed in experiment and unobservable due to the reasons described in [5], namely, the crystal torsion and other imperfections.

Of course, the applicability of suggested model depends on the possibility to restore the initial beam profile in the focusing system. This condition seems to be fulfilled in real experiments because the coefficient α is typically quite small [5]. Therefore, the projectile scattering by bent crystal does not essentially influence the beam profile. On other hand, here we paid the main attention to the saturation state, whereas this state

16

can be unreachable in practice under condition $\alpha << 1$. For this case we suggested the condition (5) to estimate the saturation possibility. Moreover, one can use common expressions (2) and (3).

Nevertheless, let consider the experimental condition [5]. The beam contained 10^9 protons in a single bunch. In the first turn 10^3 protons hit the crystal, i.e. $\alpha = 10^{-6}$. At the given α, $\beta = 0.05$ (CO) and $\eta = 0.01$ one can obtain from Eq.(5) the estimation $T \propto 10^6$ for the number of turns when saturation may be reached. Further, let suppose the proton velocity is equal 10^8 m/s and the length of storage ring 10^3 m. Hence, the time 10 s is needed to make 10^6 turns, whereas the beam lifetime was more than few minutes in experiments [5,6]. Therefore, really, one can say the saturation state exists even in this case.

It should be mentioned that the algorithm used to obtain the coefficient β implies the uniform initial distribution of projectiles at the channel cross-section. The channel cross-section has the dimension about several Angstroms, whereas the transverse beam dimension is about several mm. Usually, the beam profile is Gaussian and a bent crystal is mounted far from the beam center. Therefore, actually one can consider the uniformly distributed projectiles to calculate the coefficient β.

Finally, we would like to notice the absorber may be not symmetrical in relation to the beam direction, i.e. the cutting angle may be different at the different side of the beam. Also, absorber may be installed not in the beam direction only, but, for example, in the channeled particles motion direction. In general, other position of absorber could bring new effects related to the cutting angle.

The model suggested in this work based on simple mathematical considerations. It is not as complicated as the model [11], but it gives the results, which are in agreement in the well-known experimental data [5,6]. Therefore, this model might be useful to plan the future experiments and to simulate its results.

References

[1] D.S. Gemmel, Rev. Mod. Phys. **46**, 129 (1974).

[2] A.M. Taratin and S.A. Vorobiev, NIM B **26**, 512 (1987).

[3] A. Babaev and S.B. Dabagov, Nuovo Cimento C **34** (4) 417 (2011).

[4] A. Babaev and S.B. Dabagov, INFN LNF Preprint No LNF-11/04(P) (2011), www.lnf.infn.it/sis/preprint/detail.php?id=5248

[5] W. Scandale *et al.*, Phys. Lett. B **692**, 78 (2010).

[6] W. Scandale *et al.*, NIM B **268**, 2655 (2010).

[7] A.M. Taratin, Physics of Elementary Particles and Atomic Nuclei **29**, 437 (1998).

[8] M. Kitagawa and Y.H. Ohtsuki, Phys. Rev. B **8**, 3117, (1973).

[9] W. Scandale *et al.*, Phys. Rev. Lett. **101**, 234801 (2008).

[10] W. Scandale *et al.*, Phys. Rev. Lett. **98**, 154801 (2007).

[11] W. Scandale and A. Taratin, CERN/AT 2008-21: Dept. Report (2008).